

Original papers

Development of a LiDAR-guided section-based tree canopy density measurement system for precision spray applications

Md Sultan Mahmud^{a,b}, Azlan Zahid^{a,b}, Long He^{a,b,*}, Daeun Choi^a, Grzegorz Krawczyk^{b,c}, Heping Zhu^d, Paul Heinemann^a^a Department of Agricultural and Biological Engineering, The Pennsylvania State University, University Park, PA 16802, United States^b Fruit Research and Extension Center, The Pennsylvania State University, Biglerville, PA 17307, United States^c Department of Entomology, The Pennsylvania State University, University Park, PA 16803, United States^d Application Technology Research Unit, Agricultural Research Service, U.S. Department of Agriculture, Wooster, OH 44691, United States

ARTICLE INFO

Keywords:

Sensing
Canopy density map
Canopy volume
Precision spraying
Orchard spray
Site-specific pest management

ABSTRACT

An unmanned ground-based canopy density measurement system to support precision spraying in apple orchards was developed to precisely apply pesticides to orchard canopies. The automated measurement system was comprised of a light detection and ranging (LiDAR) sensor, an interface box for data transmission, and a laptop computer. A data processing and analysis algorithm was developed to measure point cloud indices from the LiDAR sensor to describe the distribution of tree canopy density within four sections according to the position of the trellis wires. Experiments were conducted in two orchard sites, one with GoldRush (larger trees) and the other one with Fuji (smaller trees) apple trees. Tree leaves were counted manually from each section separated by trellis wires. Field evaluation results showed a strong correlation of 0.95 ($R^2 = 89.30\%$) between point cloud data and number of leaves for the Fuji block and a correlation of 0.82 ($R^2 = 67.16\%$) was obtained for the GoldRush block. A strong correlation of 0.98 ($R^2 = 95.90\%$) was achieved in the relationship between canopy volume and number of leaves. Finally, a canopy density map was generated to provide a graphical view of the tree canopy density in different sections. Since accurate canopy density information was computed, it is anticipated that the developed prototype system can guide the sprayer unit for reducing excessive pesticide use in orchards.

1. Introduction

Conventional agriculture relies heavily on a high-level use of plant protection products, commonly known as pesticides. Pesticides play a critical role in increasing crop quality and productivity. Oerke et al. (2012) suggested that failure to use plant protection products against insects, diseases, pests, and weeds could result in up to 65% of crop yield losses. On the contrary, pesticide misuse represents a serious concern about their adverse impact on the non-targets, including humans, environment, and ecosystems (Alavanja et al., 1996; Deveau, 2009). Additionally, pesticide use caused about \$8.2 billion in annual environmental and economic losses in the United States (Pimentel & Burgess, 2014). To address this concern, the reduction of plant protection products is very important and crucial when considering agricultural sustainability and profitability.

Current development of innovative management strategies has

shown a significant reduction of pesticides and improves efficacy and safety by adopting the modern breakthrough in electronics (Ampatzidis et al., 2018). Precision spraying is one of the modern crops management strategies that assist management decisions (e.g. spraying) according to estimated variability in the field, aiming to reduce agricultural inputs. Precision spraying strategies have been utilized by researchers in the recent few decades for site-specific managements including weeds (Hunter et al., 2020), diseases (Yang, 2020), and pests (Zhong et al., 2018). The core concept of precision spraying is to adjust the spray volume by controlling nozzle flow rate.

Adjustment of the spray deposits according to the tree canopy characteristics offers the chance of decreasing pesticide use and environmental contamination (Nan et al., 2019). The tree canopy foliage plays an important role in determining the amount of spray volume required in an individual tree. However, tree canopies are not uniform in terms of density and volume. The variability of canopy foliage density is

* Corresponding author at: Department of Agricultural and Biological Engineering, The Pennsylvania State University, University Park, PA 16802, United States.
E-mail address: luh378@psu.edu (L. He).

shown in Fig. 1. Identifying tree canopy foliage density can characterize the tree structure and determine the appropriate spray volume for precise pesticide applications (Chen et al., 2012; Hu & Whitty, 2019; Wei & Salyani, 2005). It also helps to adjust the pesticide application rate, spray flow rate, and air supply volume to better manage the orchards while spraying (Gil et al., 2007; Jeon & Zhu, 2012; Llorens et al., 2010; Shen et al., 2017).

A range of techniques used for measuring tree canopy foliage density characteristics has included visible-range camera sensor (Asaei et al., 2019), ultrasonic sensor (Gil et al., 2007), spectral sensor, infrared sensor (He et al., 2011), and laser sensor (Chen et al., 2012; Liu & Zhu, 2016). Despite the considerable efforts reflected in characterizing tree canopies, challenges still exist to accurately implement the developed strategies in real-time field conditions, due to uncontrollable weather conditions and system limitations. The performance of the precision management system is significantly reduced in the field conditions due to illumination variations, wind speed and direction, and system vibrations when a camera-based sensing system is used (Asaei et al., 2019). Ultrasonic based sensing systems provide inconsistent data due to the large angle of divergence of ultrasonic waves and uncontrollable environmental conditions in fields (Zhang et al., 2018). Similarly, studies have shown the difficulty of recording accurate data using spectral and infrared sensors due to high sensitivity to the outdoor field illumination and weather conditions (Zhang et al., 2018). Conversely, laser-based sensing techniques are not affected by the outdoor field weather conditions and provide more accurate detection results (Liu & Zhu, 2016).

LiDAR (light detection and ranging) sensing is an active laser scanner-based remote sensing technique applied widely for tree canopy characterizations (Brandtberg et al., 2003; Holmgren & Persson, 2004; Hosoi & Omasa, 2006; Omasa et al., 2007). The LiDAR sensor emits an electromagnetic signal that can bounce off of the vegetation canopy enabling a view of the exterior structure and three-dimensional information of the tree. Calculation of tree canopy foliage density characteristics using a LiDAR sensor have been reported (Auat Cheein et al., 2015; Berk et al., 2020; Chakraborty et al., 2019; Hu & Whitty, 2019). Auat Cheein et al. (2015) estimated three-dimensional structure of orchard trees; in particular, real-time measurement of canopy volume and shape using a LiDAR sensor and computational geometry analysis. Results reported that the accuracy was decreased up to 30%. Underwood et al. (2016) measured the tree canopy volume using terrestrial LiDAR scanner and achieved coefficient of determination ($R^2 = 0.77$) for establishing the relationship between canopy volume and yield. Chakraborty et al. (2019) used a mobile 3D LiDAR mapping system to

measure canopy volume for apple trees and grapevines. They reported correlation values of 0.81 and 0.51 between manual and automatic measurements using Convex hull and Voxel grid methods, respectively. However, the Voxel grid method is computationally intense and is affected by the voxel size. The Convex hull method showed inferior performance compared to the Voxel grid method. Hu and Whitty (2019) evaluated a tree canopy density mapping system for a trellis-structured apple orchard where all points generated from an individual tree were included. However, a trellis-structured apple orchard may have many points produced by the wire-plane and also from the main tree trunk that need to be removed before canopy density calculation. Berk et al. (2020) established a relationship by conducting laboratory experiments for measuring tree leaf area, but low accuracies were reported. Among the studies surveyed, most researchers have tried to measure tree canopy density based on the volume of individual trees considering all points; however, the density of the whole tree cannot precisely guide the sprayer unit because the precision sprayer may have multiple nozzles on each side which need to be controlled separately. Section-based canopy density measurement leads to assessment of foliage density by dividing the tree into sections (e.g., bottom, middle, and top, etc.). The computed density information of the canopy sections can separately guide/control the corresponding nozzle facing each section. Since the precision spraying system requires nozzle flow rates to be continuously controlled during orchard spraying, the spray decision input, i.e., section-based tree canopy density information needs to be measured automatically.

The primary goal of this study was to develop an automated section-based tree canopy density measurement system for precise pesticide spraying using a LiDAR sensor. The specific objectives were to: (i) establish a relationship between the point cloud and canopy foliage without considering trellis-wires, support poles, and tree trunk (ii) predict the number of leaves in each section with the density measurement algorithm (iii) measure the tree canopy volume and generate the canopy density map for providing guideline information for variable-rate spraying.

In this study, we performed three major tasks based on LiDAR scanned data for tree canopy density and volume measurements: point cloud data acquisition, tree canopy points segmentation, and canopy density and volume measurements. Data were acquired through LiDAR integrated sensing system. A sample consensus algorithm was used to remove the ground points. Unnecessary points from tree trunks, trellis wires, and support poles were removed using a processing algorithm aimed to segment only canopy points. The canopy density and volume were measured, and canopy density map was generated. The canopy density map generated in this work provides a graphical view of tree leaves distributions in different sections, which can be used later for spraying operation in the orchards.

2. Materials and methods

2.1. Test orchards

Two orchard sites with GoldRush (site 1: 39°56'15.8"N, 77°15'21.0"W) and Fuji (site 2: 39°56'19.1"N, 77°15'17.5"W) apple varieties, located at Penn State Fruit Research and Extension Center (FREC), Biglerville, PA, USA, were used (Fig. 2). Both orchards use a trellis system to support trees, including three tiers of trellis wires and support poles. For the GoldRush block, the trees were trained as a tall spindle structure. The trees were planted in 2009 with an inter-row spacing of 6.10 m and intra-plant spacing of 1.20 m. The average tree height and width were 3.00 and 1.50 m, respectively. For the Fuji block, the trees were trained as a fruiting wall system with horizontal branches tied to the trellis wires. The trees were planted in 2016 with an inter-row spacing of 3.80 m and intra-plant spacing of 0.91 m. The average tree height and width were 2.75 and 1 m. Canopy foliage for GoldRush apple trees was denser than the Fuji variety (Fig. 2).

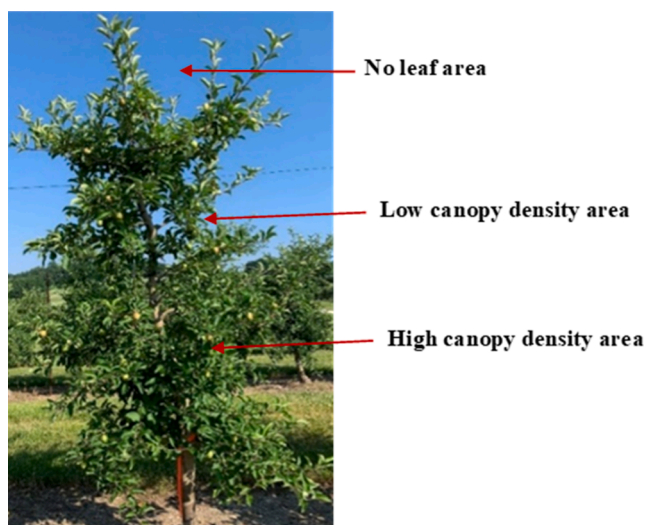


Fig. 1. Canopy foliage density variabilities within an apple tree.



Fig. 2. Test orchards (a) GoldRush apple variety (b) Fuji apple variety.

2.2. Sensor system integration and data acquisition

A point cloud data acquisition system (Fig. 3) was developed by integrating a VLP-16 LiDAR scanner (Velodyne LiDAR, San Jose, CA, USA), an interface box for data transmission and power conversion, and a 64-bit Dell 3541 laptop computer (Dell, Round Rock, TX, USA) with an Intel® i7-9750 central processing unit (CPU) running at 2.6 Gigahertz, 16 Gigabyte of Random Access Memory (RAM). The sensor was attached to an aluminum frame with a height of 1.70 m above the ground level, and the whole system was mounted on an orchard utility vehicle (Kubota, Osaka, Japan). Sixteen vertically separated beams produced by the LiDAR scanner with a range of 30° ($+15^\circ$ to -15° up and down) and angular resolution of 2° were employed to scan the apple trees in the orchards. The sensor has the ability to scan up to 0.3 million points per second with a power consumption of 8 W and an operating voltage of 9 to 32 Volt DC. The operating temperature of the sensor was -10°C to $+60^\circ\text{C}$ with an accuracy of ± 3 cm.

A series of field experiments were conducted with the data acquisition system to measure the canopy point cloud data. To evaluate the system performance, tests were conducted in the two orchard sites, including orchard site 1 on June 25th and orchard site 2 on June 30th, 2020. Both experiments were conducted during sunny weather between 4 and 5 PM with light wind. A graphical representation of the experimental setup is presented in Fig. 4. The utility vehicle was driven at the center of the row with travel speeds ranging between 5.5 and 6.5 $\text{km}\cdot\text{h}^{-1}$ during scans. The height of the trees ranged from 2.75 to 3 m and 2.2 to 2.5 m in orchard site 1 and orchard site 2, respectively at the center/middle of the tree row. The sensor to tree distances were 3.05 m and 1.90 m for scanning at orchard site 1 and orchard site 2, respectively.

Trees in a row were scanned from both sides to cover the entire canopy. In each orchard, a total of five consecutive trees located in a row were measured from both sides. The open-source VeloView software (Velodyne LiDAR, San Jose, CA, USA) was used to perform real-time visualization and recorded the live data stream. The point cloud data, namely the coordinates of the points, were stored in a laptop computer. These points represent the geometric coordinates of any object hit by the LiDAR during the scanning. A 'Packet Capture or PCAP file' contained the acquired point cloud data was collected. Files with extension '*.pcap' from two orchards were stored. Average file size was 11.9 Megabytes in our experiments. The internet protocol (IP) address of the laptop was changed before collecting the point cloud data for these experiments.

2.3. Point cloud data processing

With the acquired point cloud data, algorithms were developed to analyze tree canopy density and volume. The data processing procedure is illustrated in Fig. 5, including point cloud data pre-processing, canopy foliage estimation, canopy volume measurement, and density map generation.

2.3.1. Point cloud data pre-processing

Three-dimensional (3D) point cloud data were pre-processed using MATLAB® software (The MathWorks Inc, Natick, MA, USA) for tree canopy foliage density estimation. A Velodyne file reader function (i.e., *velodyneFileReader*) was used to read the raw scanned file (e.g., pcap) from the computer. Point cloud data were acquired for five consecutive trees in a row from two different orchards. The LiDAR sensor had a



Fig. 3. Point cloud data acquisition system was driven by a utility vehicle.

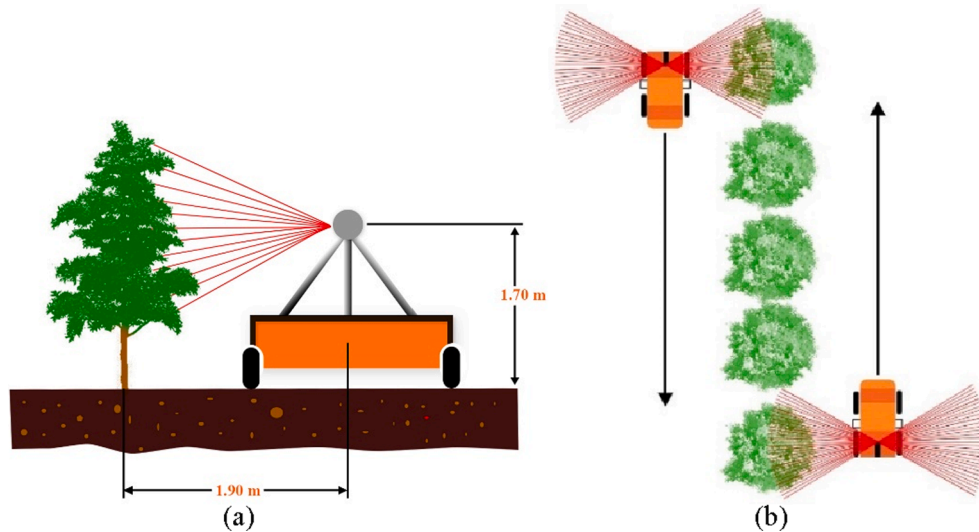


Fig. 4. Experimental setup of the LiDAR-guided system (a) utility vehicle run at the center of the row (orchard site 2) (b) consecutive five trees were scanned.

scanning speed of five frames per second. A total of 35 frames were recorded from orchard site 1 and 28 frames from orchard site 2. The LiDAR acquired about six to seven frames for one tree in orchard site 1, and four to five frames in orchard site 2 due to the smaller tree spacing, using the set driving speed. Some frames overlapped between two trees. Five separate frames were selected for each orchard site (five trees). The scanned points were then localized with the origin point at the center of the sensor. A coordinate system was defined where the x-axis was along the tree row, the y-axis was perpendicular to the tree row, and the z-axis was vertically upward along the tree trunk. Since the LiDAR was vertical to the ground during the experiments, the scanned point cloud data were orientated at 90° counter-clockwise. The transformation was conducted in two phases at the defined coordinate; in the first phase each coordinate of the data was rotated counter-clockwise around the z-axis; in the second phase, the resulting coordinate was rotated clockwise around the y-axis according to Eqs. (1) and (2).

Counter-clockwise rotation (90°) around z-axis

$$R_z(\gamma = 90^\circ) = \begin{bmatrix} \cos\gamma & -\sin\gamma & 0 & 0 \\ \sin\gamma & \cos\gamma & 0 & 0 \\ 0 & 0 & 1 & 0 \\ 0 & 0 & 0 & 1 \end{bmatrix} \quad (1)$$

Clockwise rotation (90°) around the y-axis

$$R_y(\beta = 90^\circ) = \begin{bmatrix} \cos\beta & 0 & -\sin\beta & 0 \\ 0 & 1 & 0 & 0 \\ \sin\beta & 0 & \cos\beta & 0 \\ 0 & 0 & 0 & 1 \end{bmatrix} \quad (2)$$

The transformed point cloud data included points from the trees in different rows. Therefore, a region of interest (ROI) was set to extract the targeted points from an individual tree. Targeted points were segmented by specifying an ROI and using a Kd-tree based search algorithm (Vemulapalli, 2020). The ROI of -1.5 to 1.5 m in the x-axis, -4.5 to -2.3 m in the y-axis, and -1.8 to 1.8 m in the z-axis was selected in orchard site 1. The ROI of -0.50 to 0.50 m in the x-axis, 1.5 – 2.5 m in the y-axis, and -1.8 to 1.8 m in the z-axis were used for orchard site 2. The extracted points also included the ground plane at the bottom of the targeted tree which was removed before locating the canopies in the tree. A *pcfitplane()* function using the M-estimator SAmple Consensus (MSAC) algorithm was applied to fit the plane in the 3D point cloud, which has a maximum allowable distance from an inlier point to the plane. The MSAC algorithm is a variant of the RANdom SAmple Consensus (RANSAC) algorithm. The RANSAC is an iterative method for the robust fitting of mathematical models in the presence of many data

outliers. The RANSAC was best fitted in these experiments due to the separable ground plane points from the tree canopy points. The ground plane points were then considered as outliers. The RANSAC algorithm shown in Fig. 6 was used to search the best trellis plane. A maximum distance (i.e., distance from an inlier point to the plane) of 0.15 m and the reference vector to the z-axis direction was utilized to the plane fitting for ground segmentation. The ground points were removed from the point cloud by eliminating the outlier points in the point cloud inputs.

2.3.2. Tree canopy determination

In this study, the tree canopy was defined as the tree foliage/leaves. As stated earlier, in the test orchards, there are trellis wires and poles in the tree rows. To calculate canopy foliage density and volume, the support poles and trellis wires needed to be segmented and removed. The tree trunk is another parameter responsible for increasing the number of points and was also removed. With removing the trellis wires, poles, and trunks, it was expected to provide a more precise canopy density map. To segment the trellis wires, a custom Kd-tree based nearest neighbor search algorithm to identify the isolated points was used (Vemulapalli, 2020). The isolated points selection was based on previous work by Zeng, Feng, & He (2020). A radius of 0.1 m was utilized to identify the isolated point considering the position of the trellis wire in the orchard row. This point was identified based on the estimated Euclidean distance to the trellis wire location when a point had less than four neighboring points. The trellis wires are typically situated in a plane and corresponding to one another; therefore, the isolated points must be within the same plane. No trellis plane was recognized when there were insufficient isolated points present to fit a plane, or the position of the fitted plane was not accurate. Similar to ground plane segmentation, the MSAC calculation was utilized again to fit the trellis wire lines in the trellis plane. The identified trellis wires points were then removed.

After removing the trellis wire points, the next step was to remove tree trunks and support poles from the canopy points. Typically, the position of tree trunks and support poles are both vertical and cylindrical. To segment the tree trunk and the support pole (Fig. 7), the 3D point cloud frame was partitioned into 16 2D-point sets as indicated by the laser ID (16 different beams) where only the y-z coordinating plane was used. The range of y coordinate values was defined as [Minimum Y $- 0.2$, Maximum Y $+ 0.2$]. The value of Minimum Y and Maximum Y came from the trellis plane due to the trunks and support poles found near the trellis plane. A margin constant of 0.2 m was used to ensure consideration of all trunks and support poles. Upon confirming the range

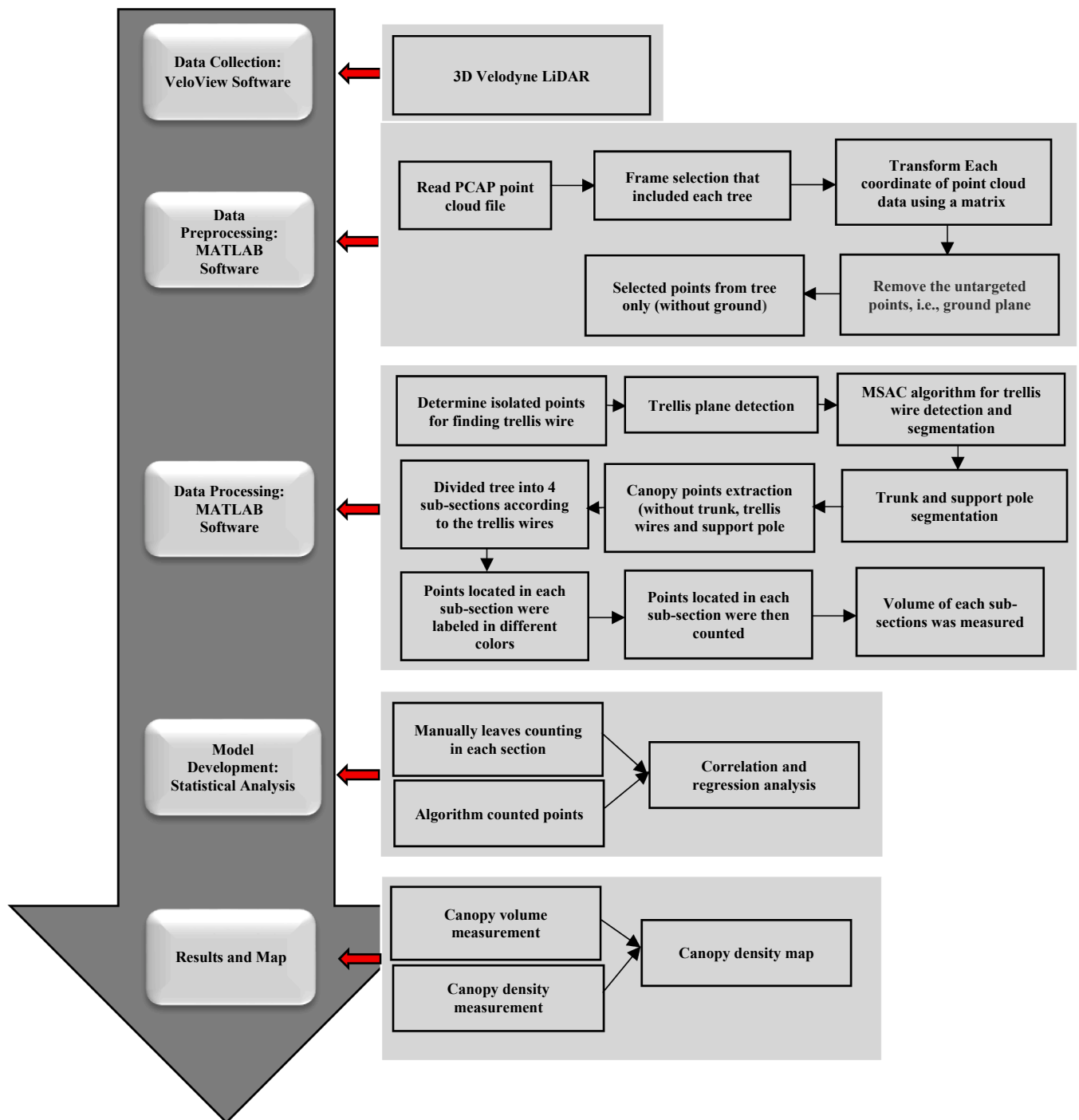


Fig. 5. Flow-chart for tree canopy density and volume measurement.

of the y coordinates, the *dbSCAN()* function was used to identify high-density clusters for determining the tree trunks and support poles. The point clusters of the tree trunks and support poles were located in a thin volume as vertically highly dense continuous points. The exposed part of each tree trunk was usually within 1 m above the ground; thus, the upper margin was set to -0.7 in the z-axis to segment tree trunks since the sensor was set at 1.7 m from the ground. After determining the high-density cluster, the *boundary()* function was used to plot the candidate clusters. Based on the height-width ratio (HW_r) and point cloud density of the candidate clusters, the tree trunk and support pole were determined (Zeng et al., 2020). The point cloud density was calculated by dividing the number of points using the area of the cluster candidate. A

density of over 3500 along with an HW_r of over 1.5 and z-axis lower than -0.5 m was used to segment the tree trunk in orchard site 1 where a density of over 2000 was used for orchard site 2. Furthermore, a density value of over 4000 and 5000 along with an HW_r of over 3 and the z-axis was 2 m applied for extraction of support pole in orchard site 1 and orchard site 2, respectively. The density value used was higher in orchard site 2 due to the larger diameter of the support poles compared to orchard site 1. Finally, the tree trunk and support pole points were removed to obtain the canopy foliage density points. Fig. 7 shows the detection of the trellis wire, pole, and tree trunk in an apple tree acquired point cloud. With segmenting and removal of these points, the remaining points represent tree canopy foliage. For GoldRush apple

<pre> 1 Step 1: int 2 Step 2: While iter < max_iter do 3 $R_i = n$ random selected points of data 4 $P_p =$ parameters of the fitted plane to R_i 5 $C_s = R_i$ 6 For (every point in data and not in R_i) 7 If (point fits P_p with a $D_e < d$) Then 8 add point to C_s 9 10 End If 11 End For 12 If (the number of points in $C_s > k$ Then 13 (a good plane is detected) 14 $T_p = P_p$ fitted to all points in C_s 15 $T_d =$ largest D_e of the fitted points 16 If ($T_e < \beta_e$) Then 17 (this plane is better than previous planes) 18 $\beta_p = T_p$ 19 $\beta_{cs} = C_s$ 20 $\beta_e = T_e$ 21 End If 22 End If 23 iter++ 24 End While </pre>	<p>Where,</p> <p>int: initialization iter : iteration R_i : random inliers P_p : plane parameters C_s: consensus set β_p : best plane β_{cs} : best consensus set β_e :best Error D_e : distance error T_p : current plane T_e: current error</p>
--	---

Fig. 6. RANSAC algorithm is written with MATLAB® software to search optimal plane.

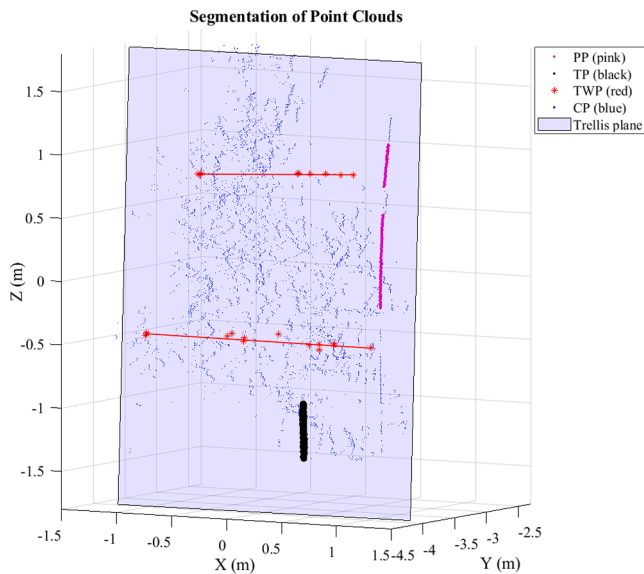


Fig. 7. Tree trunk, trellis wire and support pole detection (TP: trunk points; PP: support pole points; TWP: trellis wire points; CP: canopy points) from a Gold-Rush apple tree.

trees, only bottom section of the tree trunk was segmented due to the occlusion by leaves at the upper sections. For Fuji apple trees, the algorithm was able to detect and remove the visible trunk portions within all tree canopy sections, if they were sensed by the LiDAR sensor. Due to the smaller diameter of the tree trunks and resolution limitations of LiDAR (angular resolution of 2°), the majority of the Fuji apple tree trunk points were not acquired.

2.4. Canopy foliage point and leaf counting

To identify canopy density, the canopy foliage points were counted

from four sub-sections (Fig. 8). Determining the edge of the tree canopy is crucial to sub-divide the individual tree sections. The edge of both sides was detected using [Min x-axis, Max x-axis] functions. Upon finding the edge of an individual tree, 3D-grid coordinates were created defined by vector x, y, and z coordinates. The origin of the coordinates was located at the center of the sensor. To calculate the 3D-based canopy density, the grid was divided into four sub-sections according to the locations of three trellis wires. The heights of the sub-sections in the two orchards were: 1.22, 0.58, 0.58, and 1.22 m in Orchard site 1, and 1.17, 0.68, 0.70, and 0.44 m in orchard site 2. The grid length of the sub-sections in the x-axis direction was identified based on the edge of both sides of the tree to include the selected tree canopies. For the y-axis direction, the maximum and minimum values from the tree which had the highest depth among five trees tested were used. For the z-axis direction, the length based on trellis wire positions was used, which were $[-1.60$ to -0.38 m], $[-0.39$ to 0.20 m], $[0.21$ – 0.78 m], and $[0.79$ – 2.01 m] for sections 1 to 4 respectively in orchard site 1, and $[-1.5$ to -0.33 m], $[-0.34$ to 0.34 m], $[0.35$ – 1.05 m], and $[1.06$ – 1.50 m] for orchard site 2. To cover the whole canopy, the ranges for the y-axis was $[-4.50$ to -2.30 m] for the four sections in orchard site 1, and $[1.5$ – 2.5 m] for the orchard site 2. The range for the x-axis was [Min x-axis, Max x-axis] for each tree in both orchard sites. The grid length (i.e., in the x-axis direction) was adjusted based on the left-most and right-most of the tree canopy points; therefore the length of the x-axis varied from tree to tree, even in the same orchard site. A custom *findPointsInROI* function was used to find the indices from each sub-section followed by a MATLAB *select* function utilized for counting the number of points located in each sub-section separately. A total number of points was calculated and recorded from each sub-section from orchard site 1. A similar procedure was followed for orchard site 2.

Leaves of scanned trees were counted manually with a mechanical counter. Counting was started from the bottom section and continued to the top section. The size of the counted leaves ranged from 54 to 89 mm in length and 32 to 65 mm in width, and smaller leaves were not counted (Fig. 9). The length and width were measured at the center of the leaf, where the maximum length and width were achieved. Only the larger

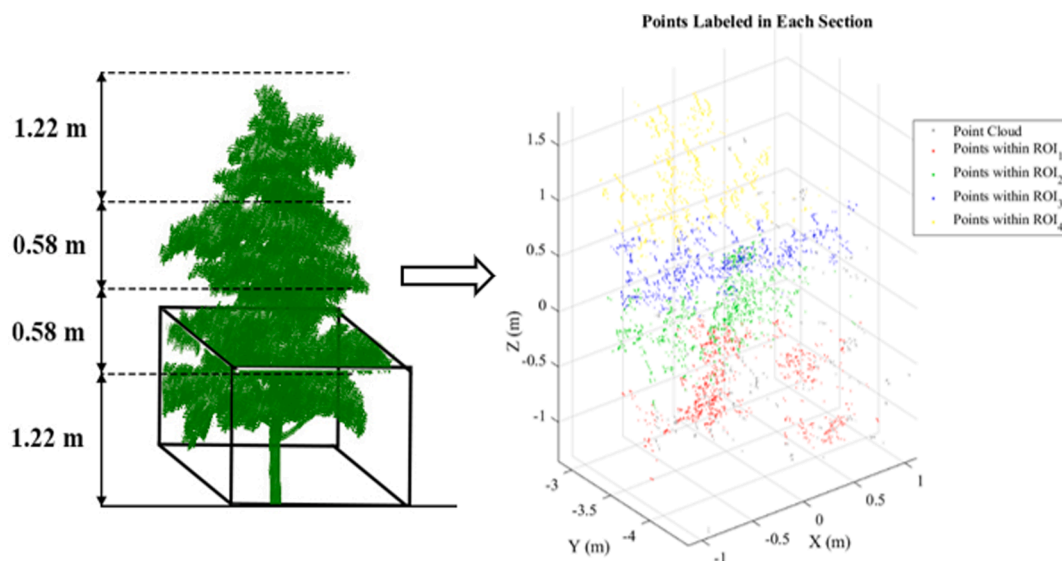


Fig. 8. Labeled canopy points in four sections of an apple tree (section 1 (bottom) to section 4 (top)).

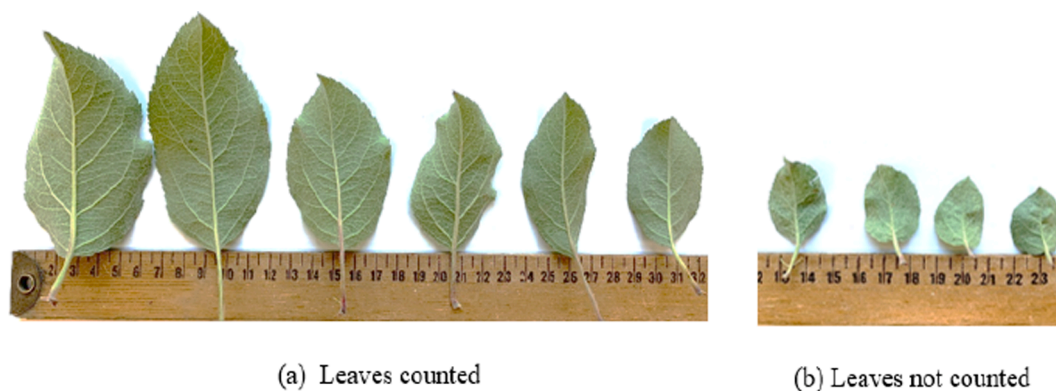


Fig. 9. Various size of apple leaves used for counting.

leaves were counted because the smaller leaves have very low possibility to be hit by the laser beam, and the large-sized leaves acquire a major portion of pesticides. Conversely, the smaller leaves intercept less quantity of chemicals than larger leaves.

The number of points counted in each sub-section was also calculated using the algorithm. The number of leaves and the number of points counted by the algorithm were then used to build a linear regression relationship. Two models were established from the two orchard sites. A linear least square was used to fit a statistical or mathematical model to the data.

2.5. Canopy density and volume measurement

2.5.1. Canopy density measurement and map

Upon removing all unnecessary points (e.g., tree trunk, trellis wires, and support pole points), the remaining points were used to calculate the canopy density of the trees. Each point cloud image from individual trees was divided into small grid areas with equal sizes of 50 cm². The number of canopy points from each grid area was counted to generate canopy density maps. Canopy points were converted to the number of leaves using the linear regression model (section 2.4) before calculating and generating the canopy density map. Finally, the canopy foliage density of each area was calculated using Eq. (3). The density map was generated by using the algorithm provided by He (2020).

$$\text{Tree Canopy Density} = \frac{N_p}{T_A} \tag{3}$$

where N_p is the number of leaves counted by the algorithm in the grid and T_A is the area of each sub-section in m².

2.5.2. Canopy volume measurement

Canopy volume is usually measured to document the size of an individual tree. An alpha shape algorithm (Fig. 11) was used to generate the 3D-shape of the individual trees, followed by volume measurements. The major advantage of the alpha shape method is that it allows for concave shapes, which is not possible with convex methods. The convex contour has a higher chance of serious overestimation due to having a fixed solution, which is not the case for concave contour (Fig. 10). The alpha shape algorithm contains several smaller regions, depending on the point set and parameters. The basic mechanism behind an alpha shape is that it starts with a Delaunay triangulation. The smaller regions are assigned with a unique label/ID, which numbers the canopy regions from the largest volume to the smallest.

2.6. Statistical analysis

Results of manual measurements (manually counted leaves) and automatically counted canopy points using the LiDAR-guided canopy density measurement system was compared separately for each orchard

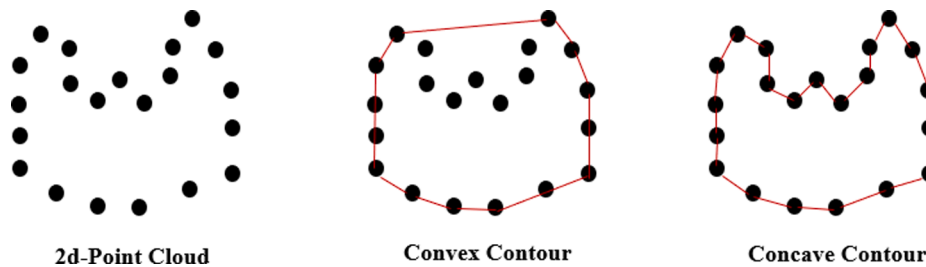


Fig. 10. Convex and concave contours of a 2d-point cloud data.

<pre> 1 Step 1: initialization 2 a = 1 3 b = 1 4 D_{K+1} = delaunay triangulation (T) 5 Step 2: For (all the elements of D_K) 6 c = Circumsphere (D_{K+1}) 7 If (c < α) Then 8 If (unique(D_K)) Then 9 D_{reg} (a) = D_K 10 a = a + 1; 11 End If 12 End If 13 c = Small Circumsphere(D_{K+1}) 14 If (c < α) Then 15 If (Is Sphere Empty(D_K)) Then 16 D_{sign} (b) = D_K 17 b = b + 1 18 End If 19 End If 20 End For </pre>	<p>Where, Input: set of point list, α Output: Alpha shape points Variables: a, b, and K are integer D and c are real</p>
--	---

Fig. 11. Alpha shape algorithm is written with MATLAB® software.

site by linear regression analysis using Minitab® 18 statistical software (Minitab® Inc., State College, PA, USA). The coefficient of determination (R^2) was also calculated for the performance evaluation of the system. We calculated percent error between the predicted number of leaves and manually counted leaves as the evaluation index for the automatic leaf counting. The percent error was defined by dividing the absolute difference of predicted leaves and manually counted leaves with manually counted leaves.

3. Results and discussion

3.1. Canopy identification in sections

The point cloud data of five consequent trees in each orchard site were processed using the developed algorithms. Figs. 12 and 13 show the tree canopies in the two test sites with and without trellis wire, poles, and tree trunks. These points were marked in different colors to

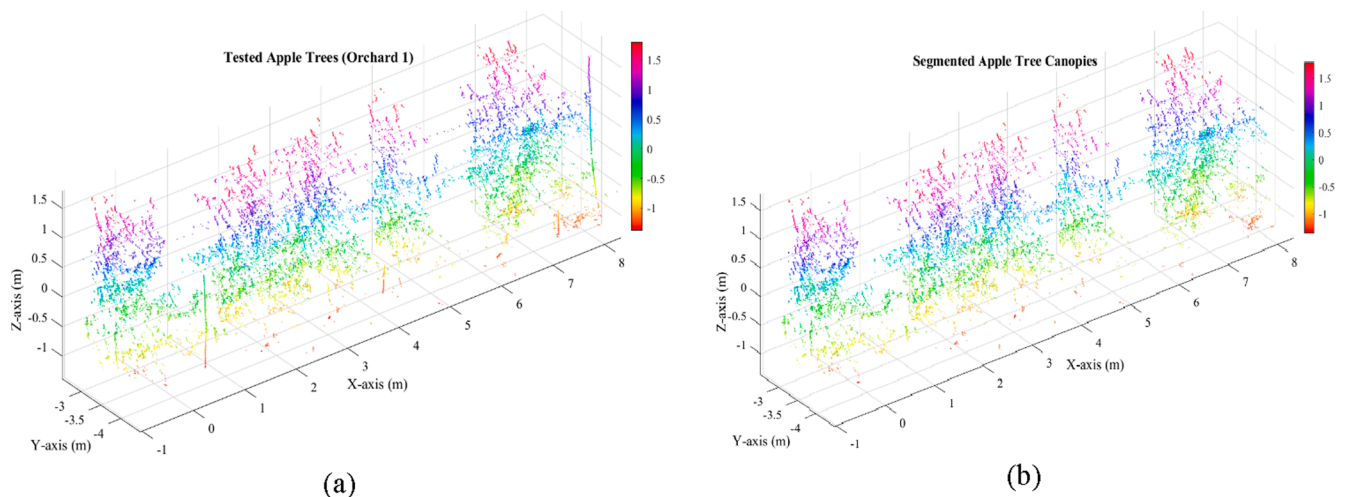


Fig. 12. Point cloud data and canopy identification in sections (orchard site 1) (a) LiDAR point cloud data after ground vegetation removal from left (tree no. 1) to the right (tree no. 5) (b) segmented tree canopy points (without tree trunk, trellis wire, and support pole).

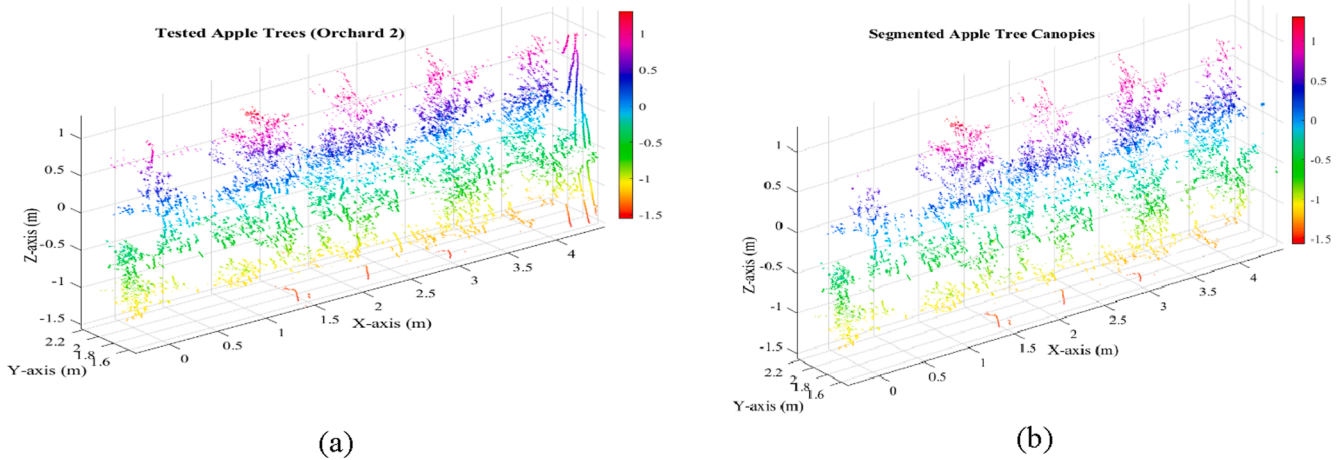


Fig. 13. Point cloud data and canopy identification in sections (orchard site 2) (a) LiDAR point cloud data after ground vegetation removal from left (tree no. 5) to the right (tree no. 1) (b) segmented tree canopy points (without tree trunk, trellis wire, and support pole).

represent four sections of tree canopy divided by the trellis wires. Figs. 12(a) and 13(a) show the point cloud data with points removed for the ground and neighboring rows. The trellis wires, poles, and tree trunks were then also removed to represent the canopy foliage, as shown in Figs. 12(b) and 13(b) for the two sites. The tree trunk and support poles were presented vertically. Not all of the tree trunks or poles were shown in the images due to being missed by the LiDAR sensor (i.e., missed by the laser beams). A potential reason for the miss was that some parts of the trunk or pole were located at the gap between laser beams, and were not acquired due to the sensor angular resolution (e.g., 2°). Tree trellis wires were also not detectable in some spots because of the occlusion caused by tree branches and leaves. Nonetheless, all acquired points from the tree trunk, trellis wires, and support poles were successfully eliminated by the algorithm to obtain only canopy points for further canopy density estimation.

3.2. Canopy density prediction model

A canopy density model was developed to predict the number of leaves in each section of the tree, which provides an idea about how much pesticide is needed in each section. Each apple tree was divided into four sections according to the position of the trellis wires. The main reason to divide sections based on trellis wires was to differentiate one section from another for manual leaf counting. Tree width was adjusted based on the minimum and maximum values of the x-axis where the average tree width of 1.5 m was calculated based on apple tree width in orchard site 1. A smaller width of 1.00 m (i.e., average) was computed for orchard site 2 due to smaller sized apple trees. Depth of the sections was fixed to 2.2 m for orchard site 1 and 1 m for orchard site 2. Two separate models were generated considering the variety and age of the

apple trees. Data gathered from five consecutive trees in each orchard site was used for the model development. The bottom tree section (i.e., section 1) had the highest numbers of leaves among the four sections (Fig. 14). The top tree section (i.e., section 4) had the fewest numbers of leaves compared to the other three sections in both of the orchard sites.

Linear regression models were developed to predict the numbers of leaves from the LiDAR point cloud data (Eq. (4) & Eq. (5)). Analysis of LiDAR point counts vs manually counted leaves suggests a fairly high correlation of 0.95 ($R^2 = 89.3\%$) reported in orchard site 2 compared to a lower correlation of 0.82 ($R^2 = 67.16\%$) calculated for orchard site 1 (Fig. 15 & Fig. 16).

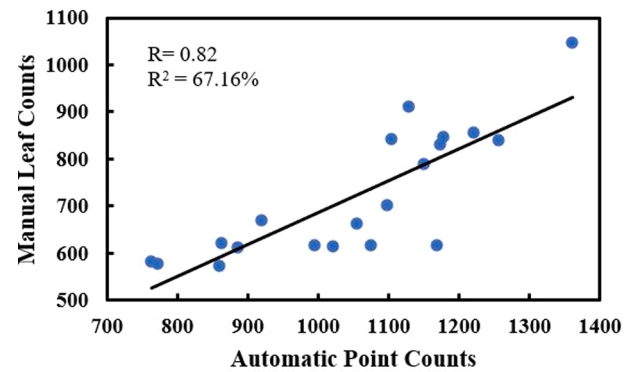


Fig. 15. Correlation between automatic point counts and manual leaf counts in orchard site 1.

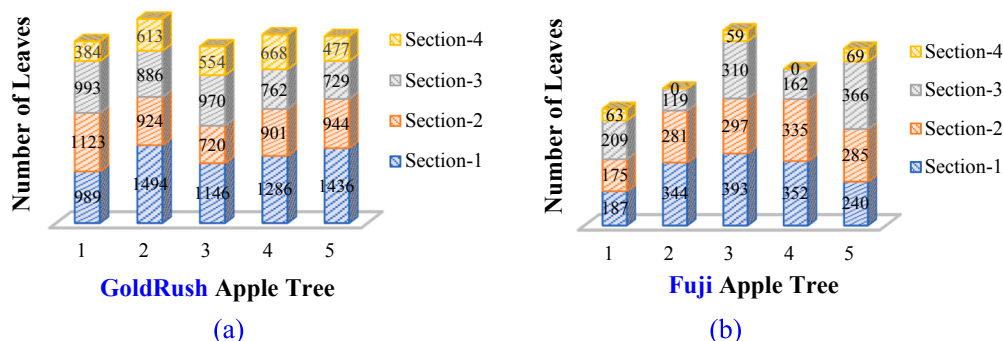


Fig. 14. Number of leaves counted from five consecutive apple trees (a) orchard site 1 (b) orchard site 2.

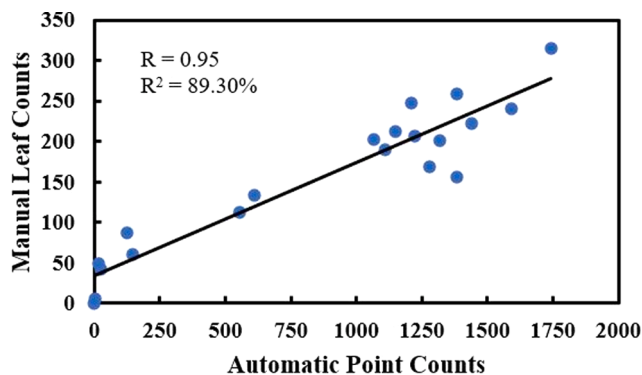


Fig. 16. Correlation between automatic point counts and manual leaf counts in orchard site 2.

$$\text{Number of leaves in orchard site 1} = 6.00 + 0.6804 \times \text{Point counted by developed algorithm} \quad (4)$$

$$\text{Number of leaves in orchard site 2} = 34.52 + 0.1391 \times \text{Point counted by developed algorithm} \quad (5)$$

In both cases, the correlation of testing apple trees was significantly higher. This was due to only one counter involved in manually counting of all the apple trees potentially reducing the error caused by inconsistent counting. However, the correlation of the orchard site 1 test was lower compared to the orchard site 2 test. One major contribution to the higher correlation in orchard site 2 lies in the lower leaf foliage density of the trees with less overlap. Manual counting may also generate some errors, especially for the high-density canopies. Berk et al. (2020) experienced similar problems for manual leaves counting resulting in poor correlations, as low as 0.27. Santoso, Tani, & Wang (2016) also reported manual counting has the potential problem of inaccurate measurement. Conversely, it was comparatively easier to count the number of leaves with the counter due to the light canopy density, which resulted in an accurate manual counting of leaves. Compared to previous studies, our study found a higher correlation due to the removal of unnecessary points from tree trunks, trellis wires, and support poles.

3.3. Tree canopy volume and number of leaves

Canopy volume was measured using an alpha shape algorithm by generating a 3D-shape of the individual trees (Fig. 17). Four different alpha values (e.g., 0.1, 0.3, 0.5, and 1) were applied for canopy volume estimation. Results showed that the lowest volume of the apple trees ranging from 0.1314 m³ to 0.4633 m³ was calculated using an alpha value of 0.1 (Table 1). Highest volumes ranging from 0.5808 m³ to 6.2668 m³ were measured with an alpha value of 1.

Relationships were built between canopy volume and the total number of manually counted leaves from the individual trees (Fig. 18). A total of 10 trees from both sites were used to configure the relationships. The highest correlation of 0.98 (R² = 95.90%) was achieved using the alpha value of 1. The alpha value of 0.3 and 0.5 also resulted in a correlation above 0.90. Conversely, the lowest correlation of 0.83 resulted from an alpha value of 0.1 because the area assigned for each point was too small. Therefore, the corresponding canopy foliage volume was also small compared to the other volumes. In a citrus tree canopy density measurement study, Wei and Salyani (2005) achieved a good correlation (R² = 0.96) between laser measurement and visual assessment. Visual assessing was performed by calculating the percentage of living material (foliage and branches) present on each tree. Another study also reported a high coefficient of determination (R²) of 0.98 during quantifying

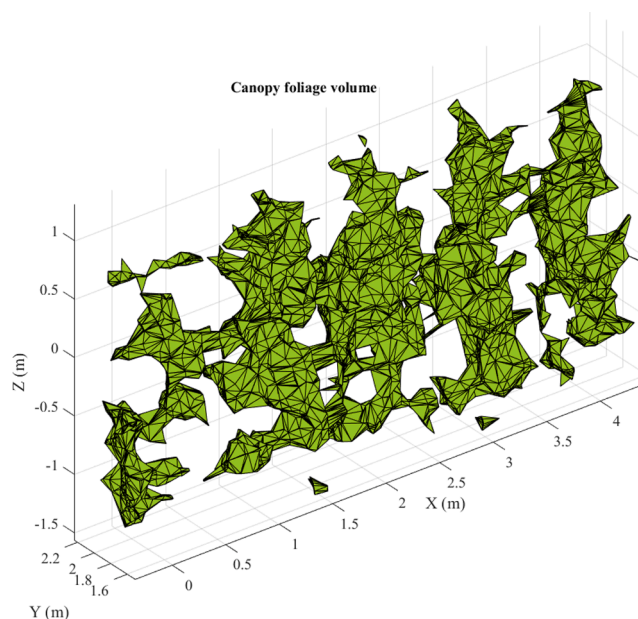


Fig. 17. Tree canopy volume measurement using the alpha value of 0.1.

Table 1
Canopy volume of apple trees by using alpha shape algorithm.

Tree No.	Alpha = 0.1volume (m ³)	Alpha = 0.3volume (m ³)	Alpha = 0.5volume (m ³)	Alpha = 1	
				(Convex hull) volume (m ³)	
Orchard site 1	1	0.3494	2.3749	3.4569	5.2639
	2	0.3663	3.0494	4.7534	5.6843
	3	0.3331	2.5446	3.9203	5.2503
	4	0.1962	1.4559	3.1410	4.3782
Orchard site 2	5	0.4633	3.3533	5.1322	6.2668
	1	0.0776	0.2809	0.3670	0.4434
	2	0.1953	0.5806	0.7265	0.8394
	3	0.1792	0.5764	0.7305	0.8766
	4	0.2003	0.6256	0.7984	0.9048
5	0.1314	0.4278	0.5161	0.5808	

canopy volume and porosity of citrus trees using the laser sensor compared with manual measurements (Ehsani & Hwan, 2008).

3.4. Canopy density map

Tree canopy density maps were generated from the acquired points and the estimated number of leaves (Equations (4) and (5)). Average processing time of a canopy density map was 2 s. Fig. 19a represents the total point density from a tree without the trunk, trellis wires, and support pole points. A canopy density map based on the acquired points was created with small grids of size 0.0567 m × 0.0884 m (width × height of one grid) (Fig. 19b). The color bar (at the right side) shows the number of canopy points per m² area. Another canopy foliage density map was generated based on the number of leaves where a grid size of 0.04 m × 0.0125 m was created to visualize the map (Fig. 19c). The color bar used in the map provides information about the number of leaves per 0.005 m² (i.e., area of one grid) area. Using the canopy density map, the number of leaves in each section of the tree can be easily calculated. The average percent error of automatically counted leaves was higher (24.44%) for orchard site 1 test than the orchard site 2 (14.21%). The less error in orchard site 2 was mainly attributed to the lower leaf foliage density.

Canopy foliage density is an important parameter for site-specific

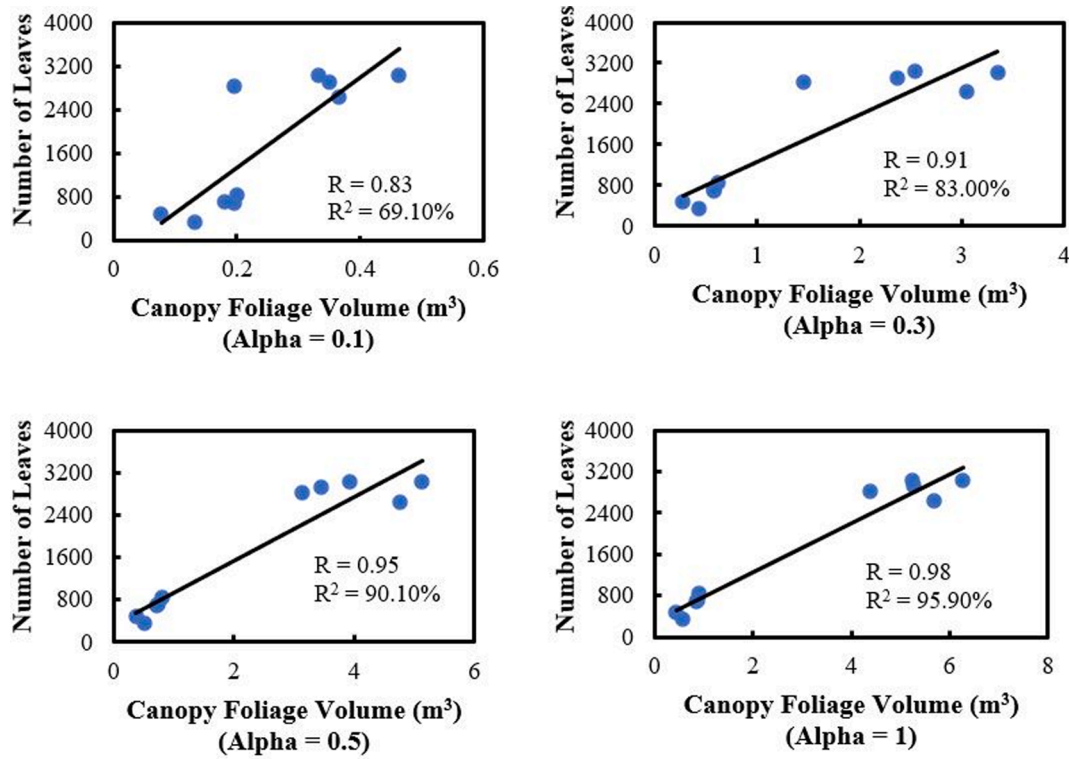


Fig. 18. Correlation between canopy foliage volume and manually counted leaves under different alpha values (0.1, 0.3, 0.5, and 1).

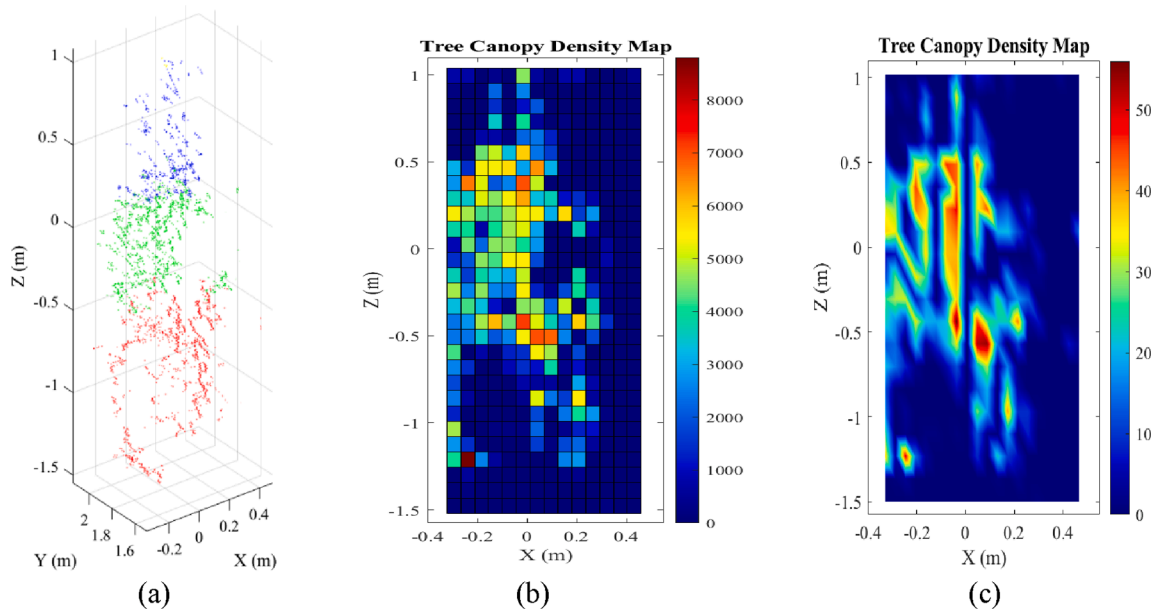


Fig. 19. Canopy foliage density map (a) tree canopy points without the trunk, trellis wires, and support pole points divided into sections (b) density map considering the number of canopy points (per m²) (c) canopy density map considering the number of leaves (per grid area).

pest management. It can provide information about where the tree has high/dense canopy density or low/light canopy density. Given the information about tree canopy density, adjustment of the nozzle flow rates is possible to guide the precision sprayer during the spraying operation. Dense canopies typically retain humidity which can lead to favorable conditions for pathogen infection and disease development (Vidal et al., 2017). Therefore, the canopy density measurement system developed in this study helps locate positions where the tree may have a higher chance of being infected. The canopy density information would also be

an indicator for controlling the flow rate of sprayer nozzles placed at different locations.

Few studies have worked on tree canopy density measurement in the past years. Underwood et al. (2016) predicted the canopy density of almond trees and reported a coefficient of determination of 0.77. The Voxel method, along with all acquired points, was used for the volume estimation where points reflected from the tree trunk, canopies, trellis wires, and support poles were also accounted for. Considering all sensed points, Chakraborty et al. (2019) predicted apple tree canopy volume

using a mobile 3D LiDAR system and achieved the highest correlation of 0.81 using the Convex hull method. Our results showed the highest correlation compared to previous studies of 0.95 using the developed canopy prediction model for the Fuji apple variety in a fruiting wall architecture. Correlation in these experiments is higher than previous studies because 1) only canopy points were considered (tree trunk, trellis wires, and support poles removed); 2) exclusion of small leaves during manual counting offered a strong correlation between manual and automatic measurements because the small canopies may have a low chance of being hit by the laser sensor.

Even though we introduced the canopy foliage prediction models for two different varieties (i.e., GoldRush and Fuji), our system is not limited to any specific apple variety. However, new models need to be created before using this system to other apple varieties considering age, shape, and size of the trees. We tested our LiDAR sensing system to orchards with flat terrain, but this system could be used in orchards with uneven (i.e., rough) and/or sloping terrain. Correction of point cloud data that may be necessary due to uneven terrain can cause deviations of the angular orientation of the LiDAR sensor during scanning (Palleja et al., 2010). In future studies, we will conduct our experiments in the uneven terrain where an IMU and GPS will be integrated with the LiDAR sensing system for canopy foliage density measurement.

Although a considerable number of studies evaluated the tree canopy characteristics (i.e., tree height, width, leaf area, etc.), the accurate site-specific management (i.e., variable-rate applications) in the orchards was a major concern until an experimental real-time laser-guided variable-rate sprayer was developed by Chen et al. (2012). However, this variable-rate sprayer did not exclude trunks, trellis wires, and support poles in tree canopy characterizations and sprayed them as the targets. The best pest management practices require more accurate and precise canopy information in reducing chemical application, especially during spraying young or sparse foliage trees. Several attempts were reported to measure leaf area density (i.e., area covered by leaves or leaf wall area) for precision spraying in the tree fruits (Berk et al., 2020; Hosoi & Omasa, 2006; Shen et al., 2017), but the leaf orientation angle can greatly affect the accuracy of these type of measurements in real-time field conditions. Different leaves have different angles that can easily affect the measurement of the leaf wall area and cause errors (Jejić et al., 2011). We measured canopy density based on tree sections where leaf orientation angle cannot affect the performance of the measurement unless other leaves fully occlude the leaf. When a substantial portion of a leaf is visible, there might be a higher chance of being hit by the laser beam, and it would then be considered as a canopy point. The tested trees were in high-density structures with relatively narrow canopy. The developed measurement system achieved fairly high correlation between manually and automatically counted leaves. While for large trees with more branch overlapping, the effectiveness of the system would need to be further investigated. Another major contribution of this study is that we calculated section-based canopy density which is essential to control each nozzle separately according to the measurements. Previous studies were only concerned about leaf area and volume of the whole tree, which cannot minimize spray drift adequately during pesticide spraying. Density information calculated from the number of points/leaves will be a good aid for precision spraying, which will be tested in future work.

4. Conclusions

Apple tree canopy density was assessed using a ground-based LiDAR guided sensing system. Point cloud data were acquired from two orchard sites with GoldRush and Fuji apple varieties. A processing algorithm was scripted in the MATLAB® programming environment. Experiments were conducted with T-trellis structured orchards; therefore, tree trunk, trellis wires, and support poles were extracted to separate only the canopy points from the acquired data. Apple leaves were counted manually by a counter, and also automatically estimated by the developed algorithm.

Two apple tree leaves prediction models were developed for two varieties with different sizes and shapes. The canopy volume of individual apple trees was measured using an alpha shape algorithm applying different values (0.1, 0.3, 0.5, and 1). The relationship of the canopy volume and manually counted leaves was established. Results reported a strong correlation of 0.95 between manually counted leaves and acquired point cloud data from a LiDAR sensor using Fuji apple tree data (smaller canopy). In comparison, the correlation dropped to 0.82 using the GoldRush variety (larger canopy) during field evaluation. Canopy volume measured by using the alpha shape algorithm showed a strong relationship with manually counted leaves with a correlation up to 0.98 using an alpha value of 1. Additionally, the canopy density maps can pinpoint high, moderate, and low density, and also no leaf regions within the apple trees, which should be able to guide precision management systems. This study was conducted in flat terrain surfaces; in the future, we will conduct experiments in uneven terrain integrating an IMU and GPS to this LiDAR sensing system. Point cloud position will be corrected based on the IMU readings and a GPS for the georeferenced location. The canopy density information will be used for precision spraying operations by adjusting the nozzle flow rate based on the appearance of the canopy in each tree section.

CRedit authorship contribution statement

Md Sultan Mahmud: Conceptualization, Investigation, Methodology, Validation, Writing - original draft. **Azlan Zahid:** Investigation, Methodology, Validation. **Long He:** Conceptualization, Supervision, Writing - review & editing, Funding acquisition. **Daeun Choi:** Supervision, Writing - review & editing. **Grzegorz Krawczyk:** Supervision, Writing - review & editing. **Heping Zhu:** Supervision, Writing - review & editing. **Paul Heinemann:** Supervision, Writing - review & editing.

Declaration of Competing Interest

The authors declare that they have no known competing financial interests or personal relationships that could have appeared to influence the work reported in this paper.

Acknowledgement

This study was supported in part by United States Department of Agriculture (USDA)'s National Institute of Food and Agriculture (NIFA) Federal Appropriations under Project PEN04653 and Accession No. 1016510, a USDA NIFA Crop Protection and Pest Management Program (CPM) competitive grant (Award No. 2019-70006-30440), and a Northeast Sustainable Agriculture Research and Education (SARE) Graduate Student Grant GNE20-234-34268. The authors would like to give special thanks to Xiaohu Jiang (visiting scholar) and Mingsen Huang (visiting scholar) for their assistance during the field experiments.

References

- Alavanja, M.C., Sandler, D.P., McMaster, S.B., Zahm, S.H., McDonnell, C.J., Lynch, C.F., Blair, F.A., 1996. The agricultural health study. *Environ. Health Perspect.* 104 (4), 362–369.
- Ampatzidis, Y., Kiner, J., Abdolee, R., Ferguson, L., 2018. Voice-controlled and wireless solid set canopy delivery (VCW-SSCD) system for mist-cooling. *Sustainability (Switzerland)* 10 (2), 421.
- Asaei, H., Jafari, A., Loghavi, M., 2019. Site-specific orchard sprayer equipped with machine vision for chemical usage management. *Comput. Electron. Agric.* 162, 431–439.
- Auat Cheein, F.A., Guivant, J., Sanz, R., Escolà, A., Yandún, F., Torres-Torriti, M., Rosell-Polo, J.R., 2015. Real-time approaches for characterization of fully and partially scanned canopies in groves. *Comput. Electron. Agric.* 118, 361–371.
- Berk, P., Stajniko, D., Belsak, A., Hocevar, M., 2020. Digital evaluation of leaf area of an individual tree canopy in the apple orchard using the lidar measurement system. *Comput. Electron. Agric.* 169, 105158.
- Brandtberg, T., Warner, T.A., Landenberger, R.E., McGraw, J.B., 2003. Detection and analysis of individual leaf-off tree crowns in small footprint, high sampling density

- lidar data from the eastern deciduous forest in North America. *Remote Sens. Environ.* 85 (3), 290–303.
- Chakraborty, M., Khot, L.R., Sankaran, S., Jacoby, P.W., 2019. Evaluation of mobile 3D light detection and ranging based canopy mapping system for tree fruit crops. *Comput. Electron. Agric.* 158, 284–293.
- Chen, Y., Zhu, H., Ozkan, H.E., 2012. Development of a variable-rate sprayer with laser scanning sensor to synchronize spray outputs to tree structures. *Trans. ASABE* 55 (3), 773–781.
- Deveau, J., 2009. Six Elements of Effective Spraying in Orchards and Vineyards. Ministry of Agriculture, Food and Rural Affairs, Ontario.
- Ehsani, R., Hwan, L.E.E., 2008. A measurement system for quantifying citrus foliage volume and porosity. *Tarım Makinaları Bilimi Dergisi* 4 (4), 333–338.
- Gil, E., Escolà, A., Rosell, J.R., Planas, S., Val, L., 2007. Variable rate application of plant protection products in vineyard using ultrasonic sensors. *Crop Prot.* 26 (8), 1287–1297.
- He, X., Zeng, A., Liu, Y., Song, J., 2011. Precision orchard sprayer based on automatically infrared target detecting and electrostatic spraying techniques. *Int. J. Agric. Biol. Eng.* 4 (1), 35–40.
- He, C., 2020. `densityplot(x,y,varargin)` (<https://www.mathworks.com/matlabcentral/fileexchange/65166-densityplot-x-y-varargin>), MATLAB Central File Exchange. Retrieved August 5, 2020.
- Holmgren, J., Persson, Å., 2004. Identifying species of individual trees using airborne laser scanner. *Remote Sens. Environ.* 90 (4), 415–423.
- Hosoi, F., Omasa, K., 2006. Voxel-based 3-D modeling of individual trees for estimating leaf area density using high-resolution portable scanning lidar. *IEEE Trans. Geosci. Remote Sens.* 44 (12), 3610–3618.
- Hu, M., Whitty, M., 2019. An evaluation of an apple canopy density mapping system for a variable-rate sprayer. *IFAC-PapersOnLine* 52 (30), 342–348.
- Hunter, J.E., Gannon, T.W., Richardson, R.J., Yelverton, F.H., Leon, R.G., 2020. Integration of remote-weed mapping and an autonomous spraying unmanned aerial vehicle for site-specific weed management. *Pest Manag. Sci.* 76 (4), 1386–1392.
- Jejić, V., Godeša, T., Hocevar, M., Širok, B., Malneršić, A., Štancar, A., Stajanko, D., 2011. Design and testing of an ultrasound system for targeted spraying in orchards. *Strojnicki Vestnik/J. Mech. Eng.* 57 (7–8), 587–598.
- Jeon, H.Y., Zhu, H., 2012. Development of a variable-rate sprayer for nursery liner applications. *Trans. ASABE* 55 (1), 303–312.
- Liu, H., Zhu, H., 2016. Evaluation of a laser scanning sensor in detection of complex-shaped targets for variable-rate sprayer development. *Trans. ASABE* 59 (5), 1181–1192.
- Llorens, J., Gil, E., Llop, J., Escolà, A., 2010. Variable rate dosing in precision viticulture: use of electronic devices to improve application efficiency. *Crop Prot.* 29 (3), 239–248.
- Nan, Y., Zhang, H., Zheng, J., Bian, L., Li, Y., Yang, Y., Ge, Y., 2019. Estimating leaf area density of *Osmanthus* trees using ultrasonic sensing. *Biosyst. Eng.* 186, 60–70.
- Oerke, E.C., Dehne, H.W., Schönbeck, F., Weber, A., 2012. Crop production and crop protection: estimated losses in major food and cash crops.
- Omasa, K., Hosoi, F., Konishi, A., 2007. 3D lidar imaging for detecting and understanding plant responses and canopy structure. *J. Exp. Bot.* 58 (4), 881–898.
- Palleja, T., Tresanchez, M., Teixido, M., Sanz, R., Rosell, J.R., Palacin, J., 2010. Sensitivity of tree volume measurement to trajectory errors from a terrestrial lidar scanner. *Agric. For. Meteorol.* 150 (11), 1420–1427.
- Pimentel, D., Burgess, M., 2014. Environmental and economic costs of the application of pesticides primarily in the United States. In: *Integrated Pest Management*, pp. 47–71.
- Santoso, H., Tani, H., Wang, X., 2016. A simple method for detection and counting of oil palm trees using high-resolution multispectral satellite imagery. *Int. J. Remote Sens.* 37 (21), 5122–5134.
- Shen, Y., Zhu, H., Liu, H., Chen, Y., Ozkan, E., 2017. Development of a laser-guided, embedded-computer-controlled, air-assisted precision sprayer. *Trans. ASABE* 60 (6), 1827–1838.
- Underwood, J.P., Hung, C., Whelan, B., Sukkarieh, S., 2016. Mapping almond orchard canopy volume, flowers, fruit and yield using lidar and vision sensors. *Comput. Electron. Agric.* 130, 83–96.
- Vemulapalli, P., 2020. `Kdtree implementation in matlab` (<https://www.mathworks.com/matlabcentral/fileexchange/26649-kdtree-implementation-in-matlab>), MATLAB Central File Exchange. Retrieved April 19, 2020.
- Vidal, T., Boixel, A.L., Durand, B., de Vallavieille-Pope, C., Huber, L., Saint-Jean, S., 2017. Reduction of fungal disease spread in cultivar mixtures: Impact of canopy architecture on rain-splash dispersal and on crop microclimate. *Agric. For. Meteorol.* 246, 154–161.
- Wei, J., Salyani, M., 2005. Development of a laser scanner for measuring tree canopy characteristics: Phase 2. Foliage density measurement. *Trans. ASAE* 48 (4), 1595–1601.
- Yang, C., 2020. Remote sensing and precision agriculture technologies for crop disease detection and management with a practical application example. *Engineering* 6 (5), 528–532.
- Zeng, L., Feng, J., He, L., 2020. Semantic segmentation of sparse 3D point cloud based on geometrical features for trellis-structured apple orchard. *Biosyst. Eng.* 196, 46–55.
- Zhang, Z., Wang, X., Lai, Q., Zhang, Z., 2018. Review of variable-rate sprayer applications based on real-time sensor technologies. In: *Automation in Agriculture: Securing Food Supplies for Future Generations*, p. Ch. 4, 53–79.
- Zhong, Y., Gao, J., Lei, Q., Zhou, Y., 2018. A vision-based counting and recognition system for flying insects in intelligent agriculture. *Sensors (Switzerland)* 18 (5), 1489.